

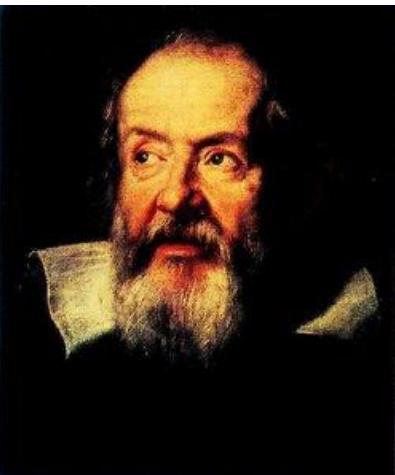
# 同时在位形空间和尺度域探究星系形成物理对宇宙物质分布的影响

王云



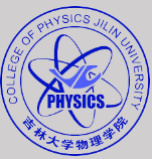
吉林大学物理学院  
COLLEGE OF PHYSICS · JILIN UNIVERSITY

邮 箱: yunw@jlu.edu.cn  
学术主页: wangyun1995.github.io



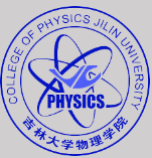
2024 Annual Meeting of the Gravitational and Relativistic  
Astrophysics Branch of the Chinese Physical Society  
中国物理学会引力与相对论天体物理分会  
2024年学术年会

The Sixth GALILEO-XU GUANGQI Meeting  
第六届伽利略-徐光启会议

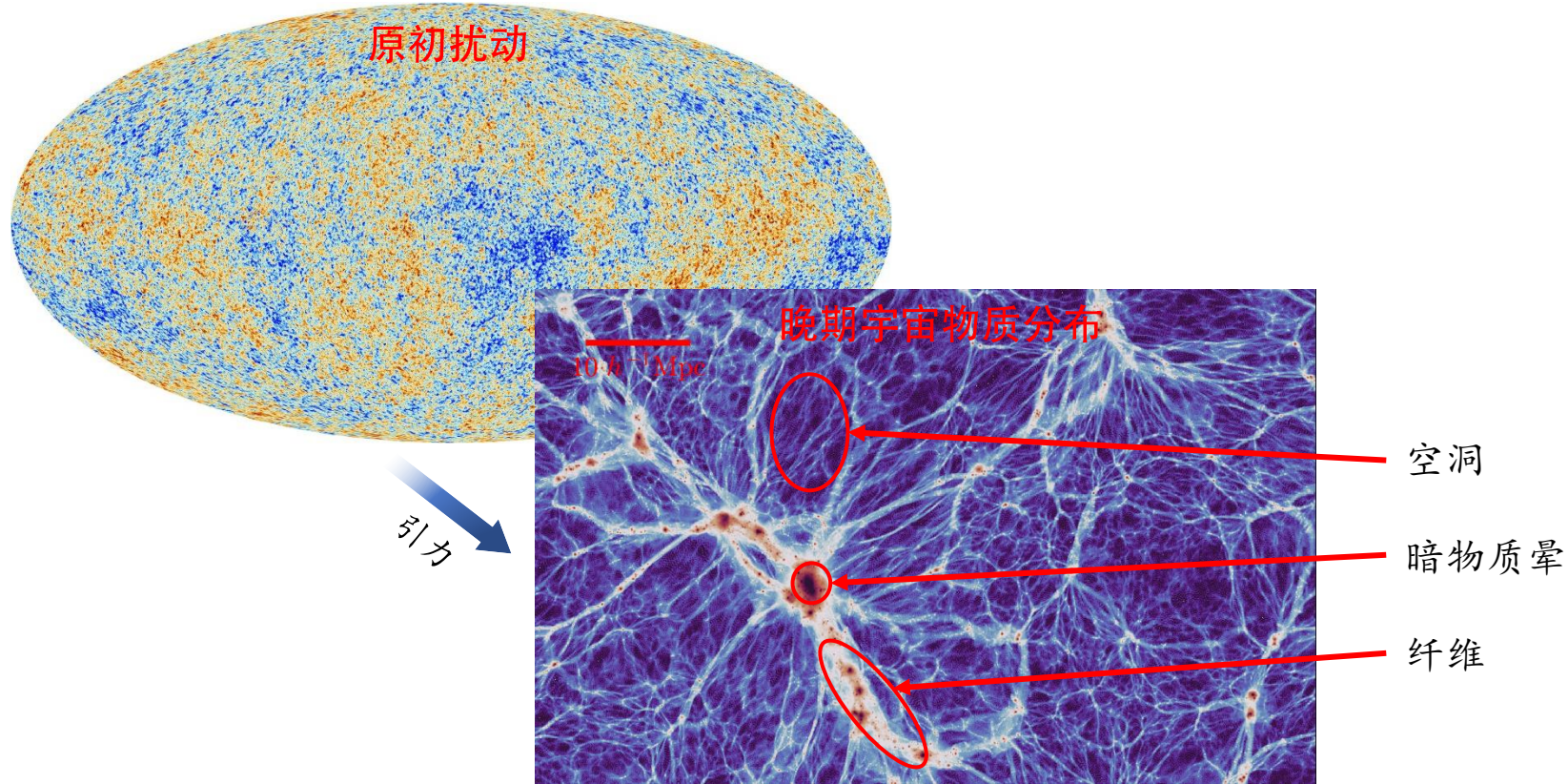


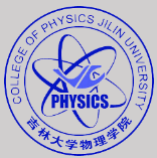
# 目录

- 物质分布中的重子效应
- 重子效应的研究现状
- 重子效应的空间-尺度分析
- 结果和结论

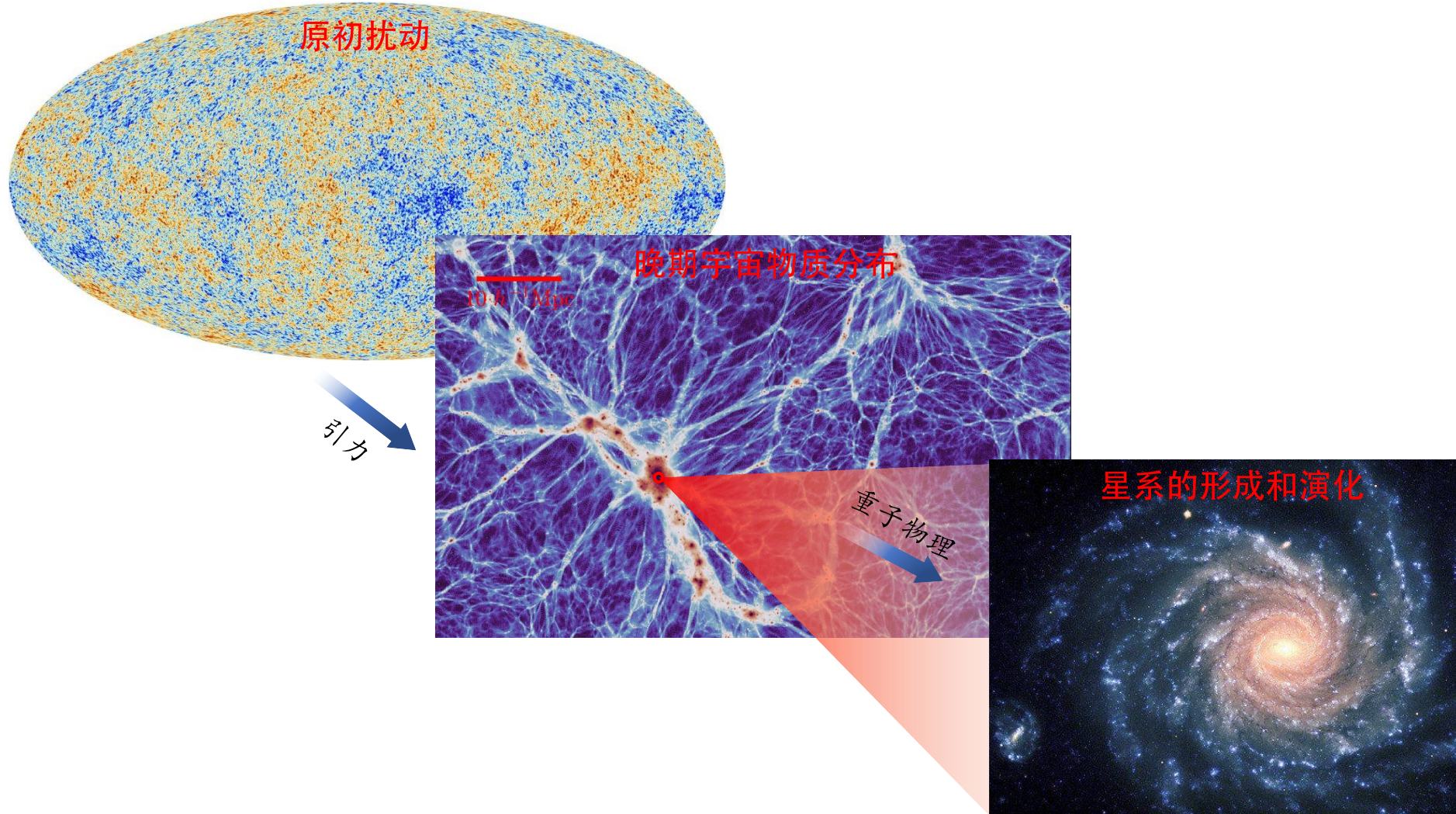


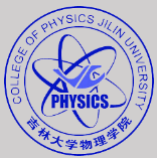
# 物质分布中的重子效应



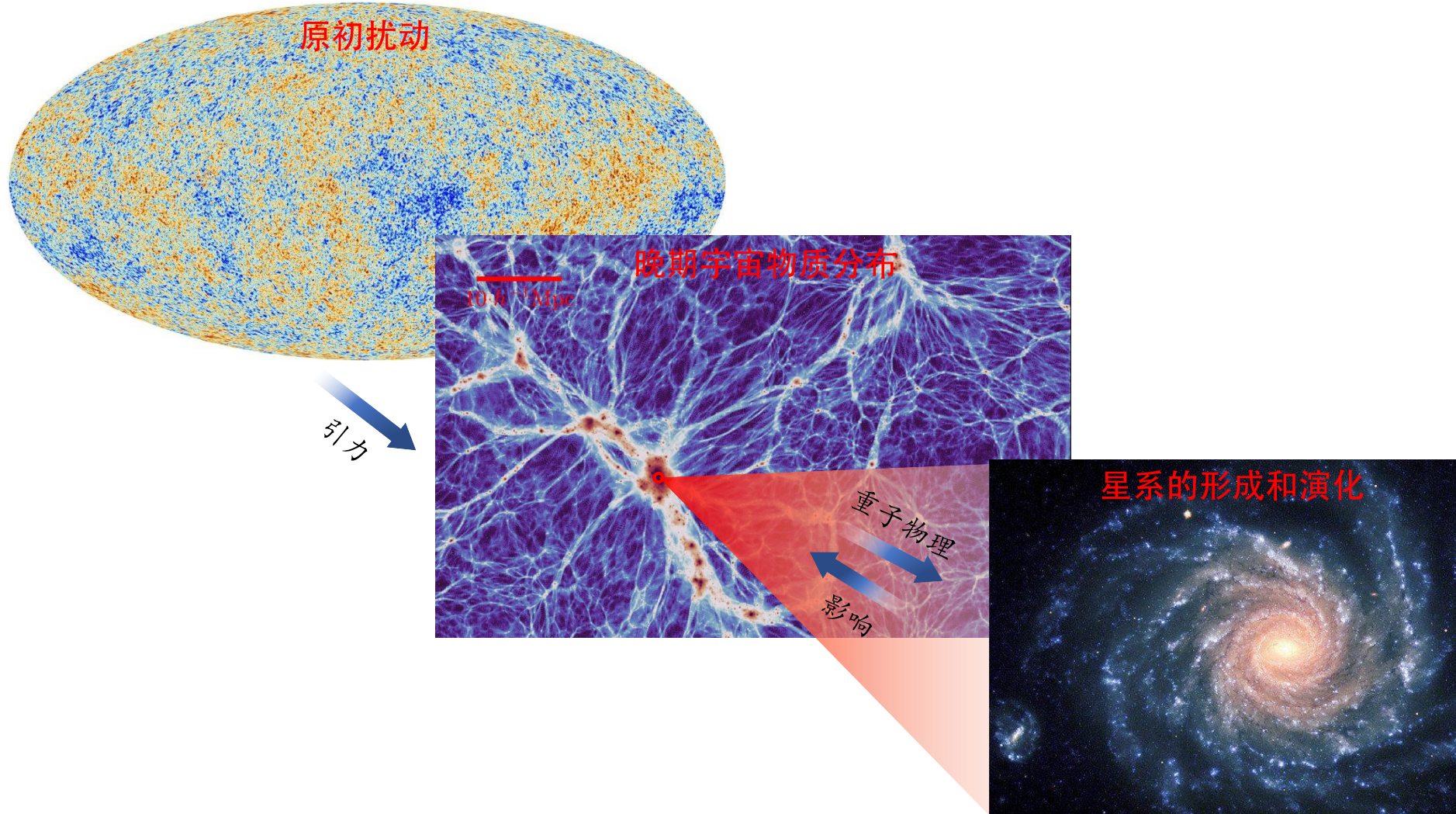


# 物质分布中的重子效应

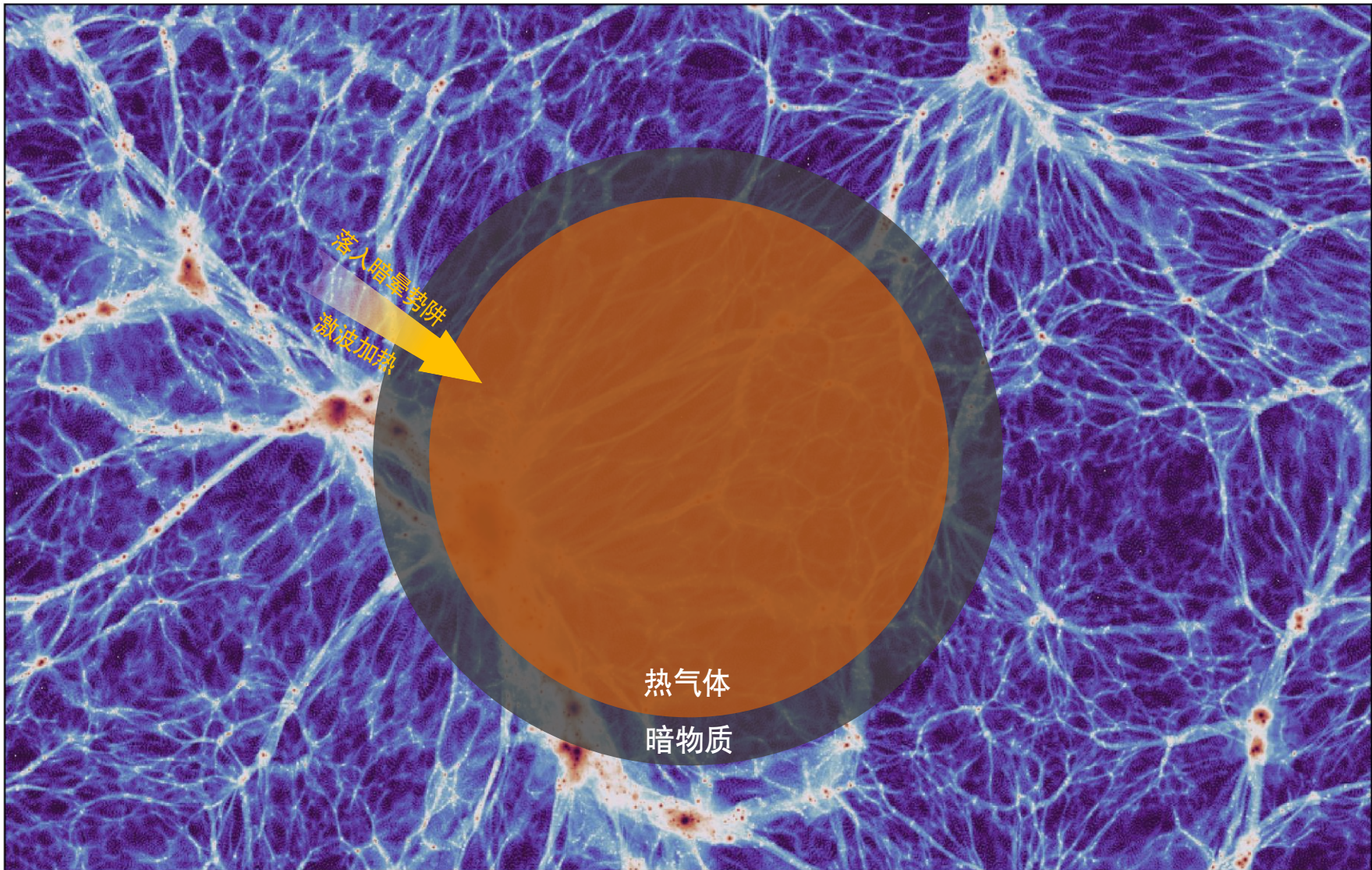




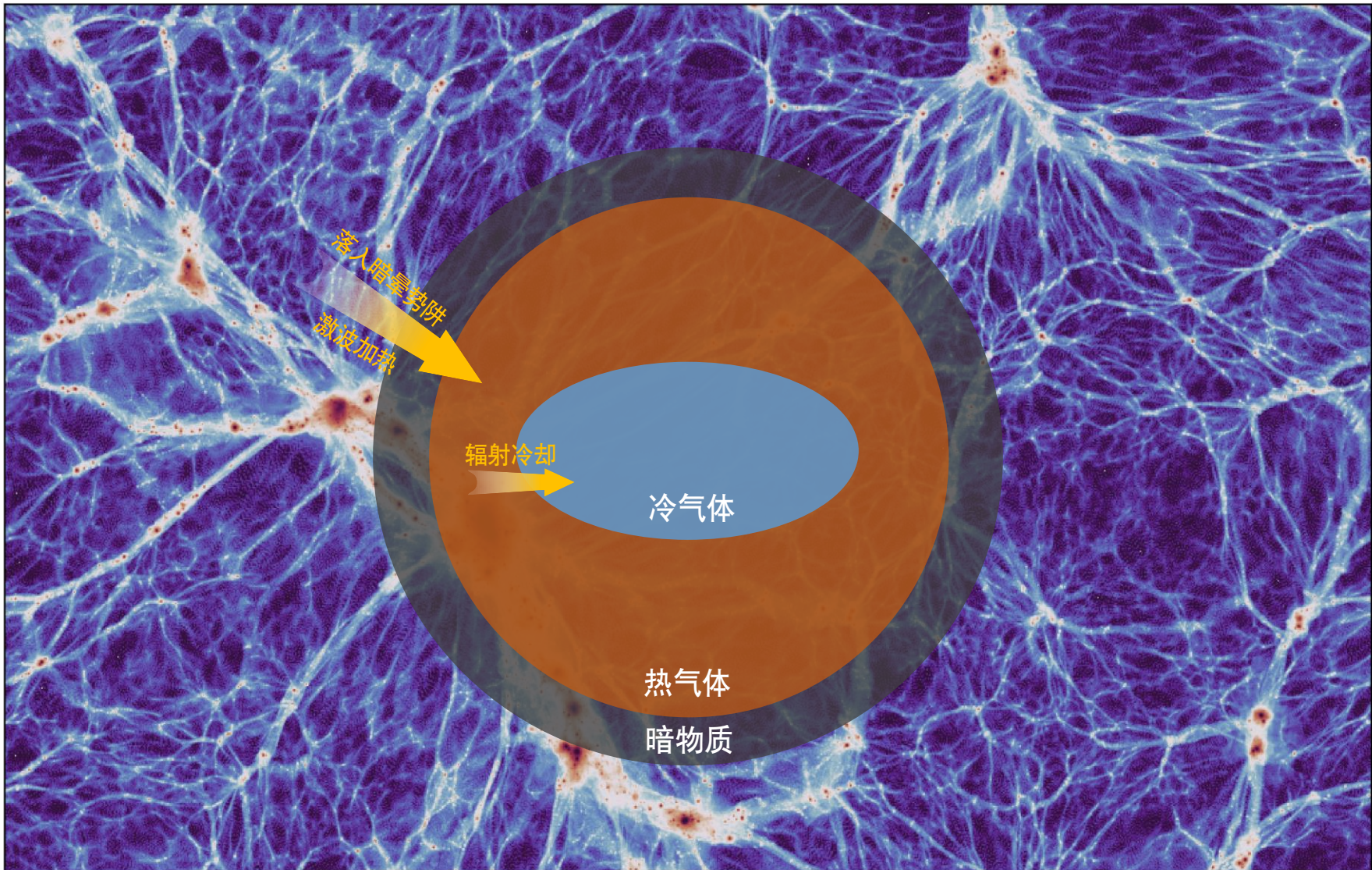
# 物质分布中的重子效应



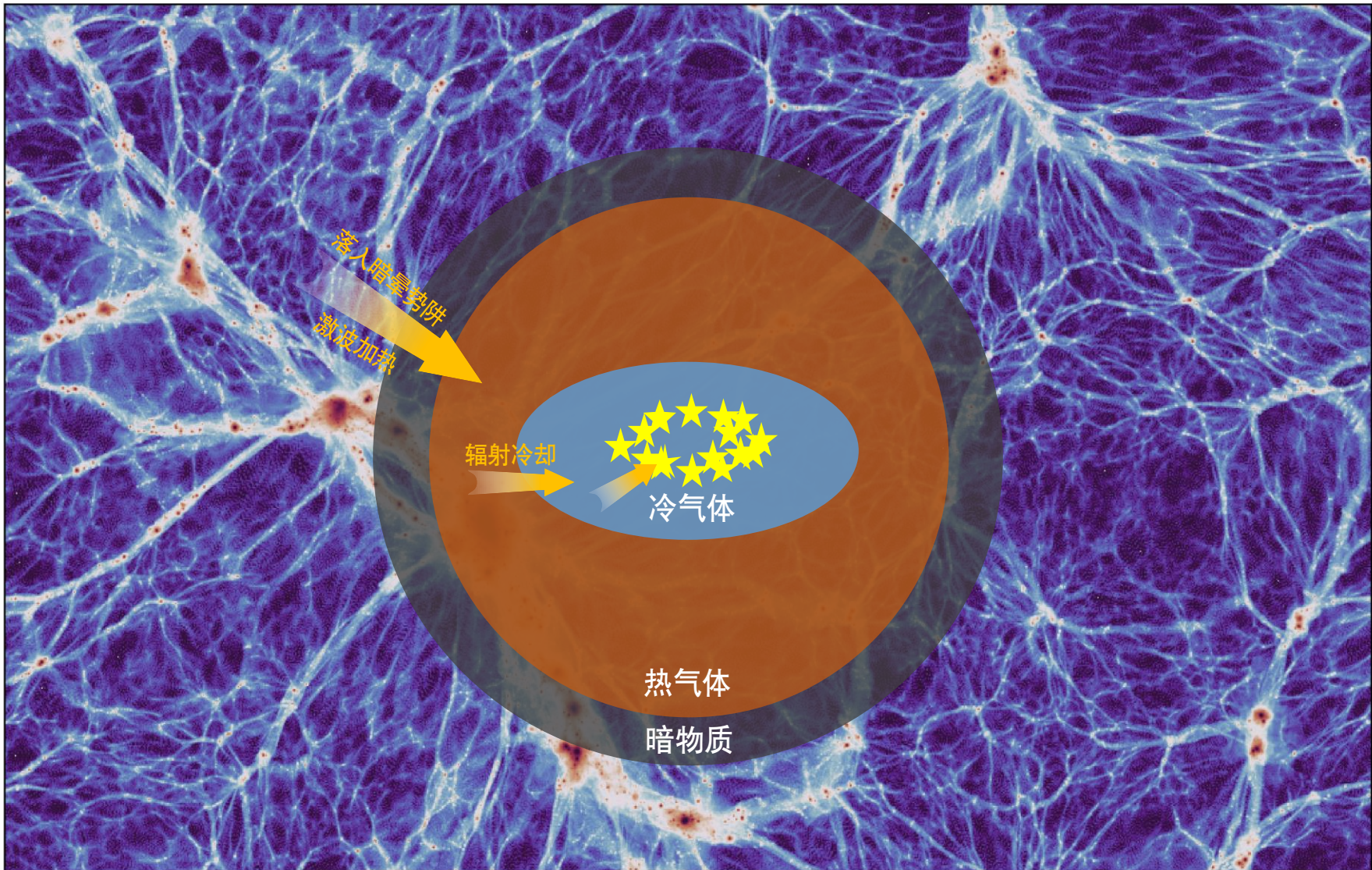
# 物质分布中的重子效应



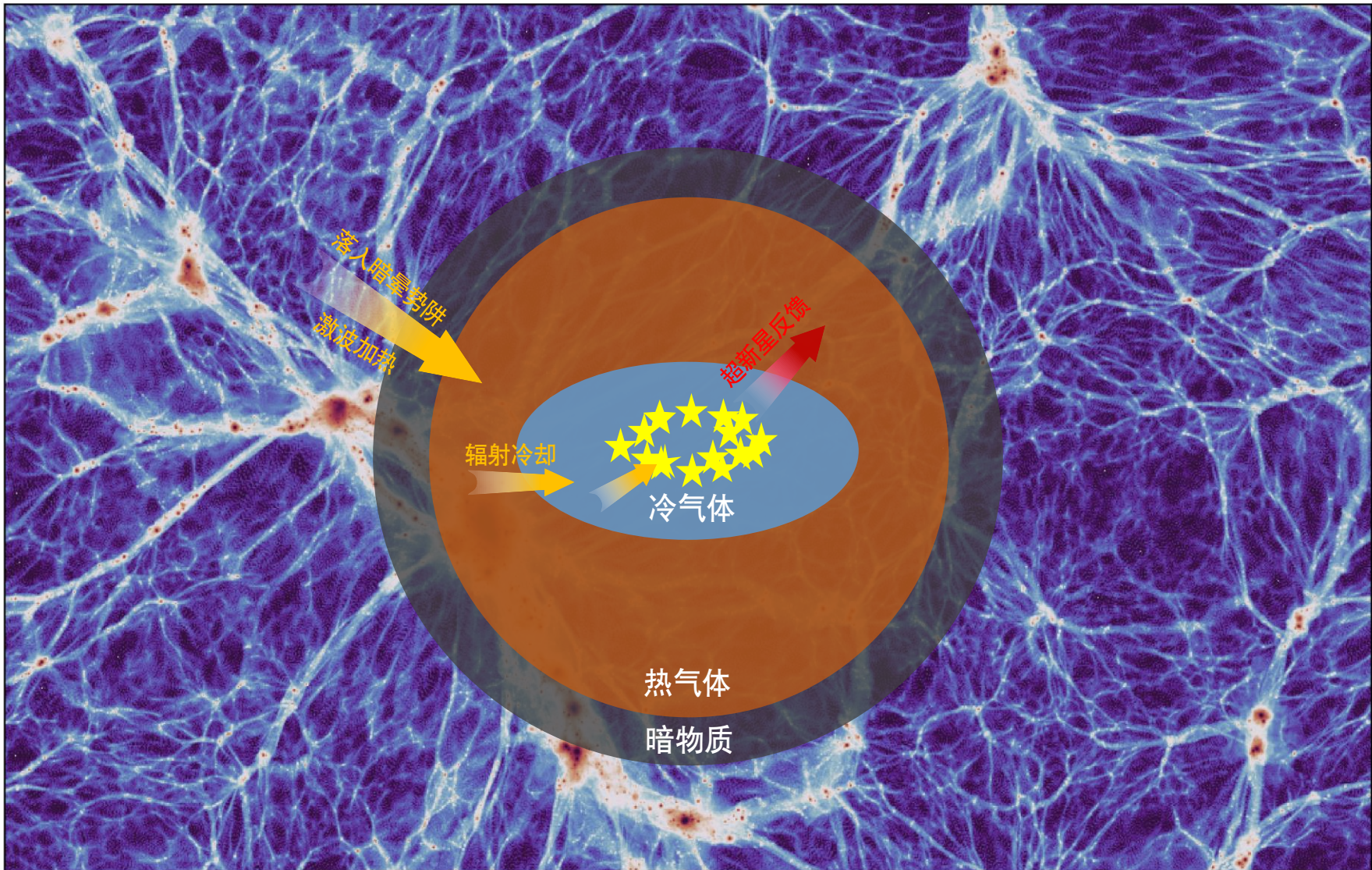
# 物质分布中的重子效应



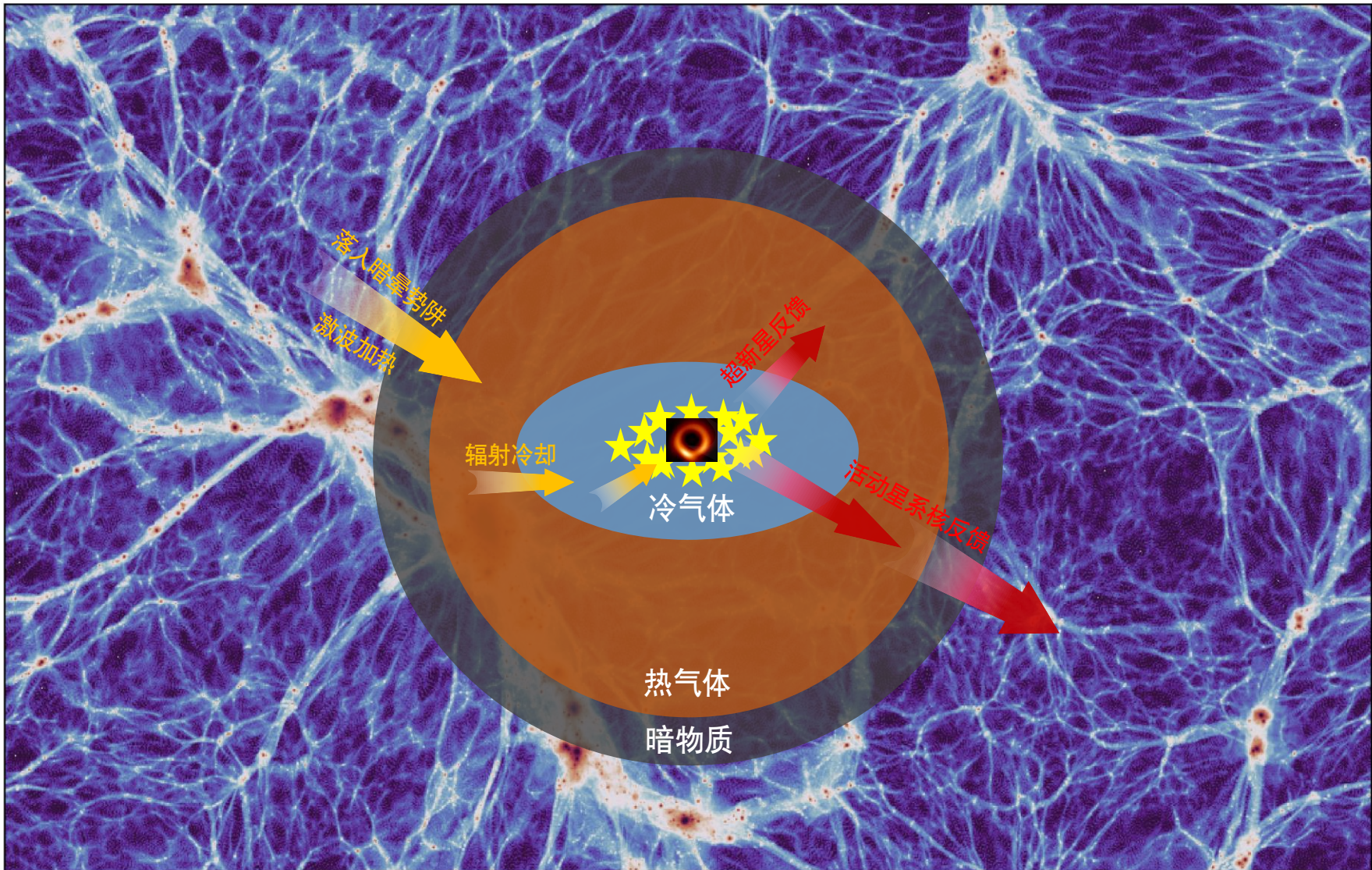
# 物质分布中的重子效应



# 物质分布中的重子效应



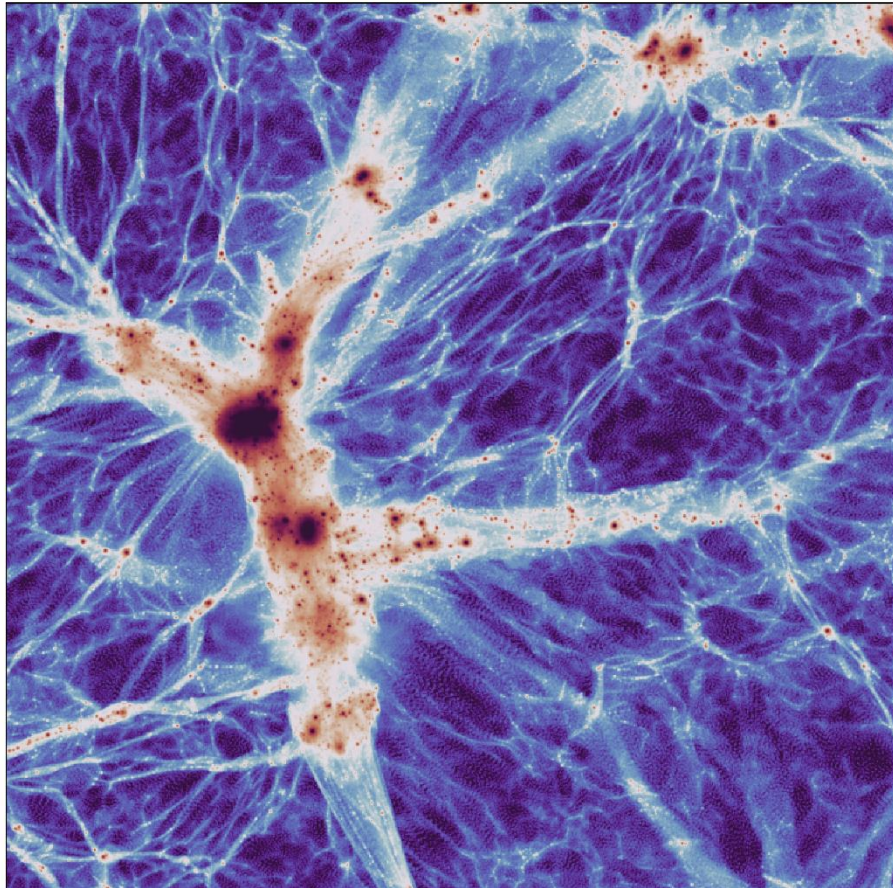
# 物质分布中的重子效应



# 重子效应的研究现状

流体动力学 (Hydro) 模拟

暗物质+重子物质(气体、恒星和黑洞)

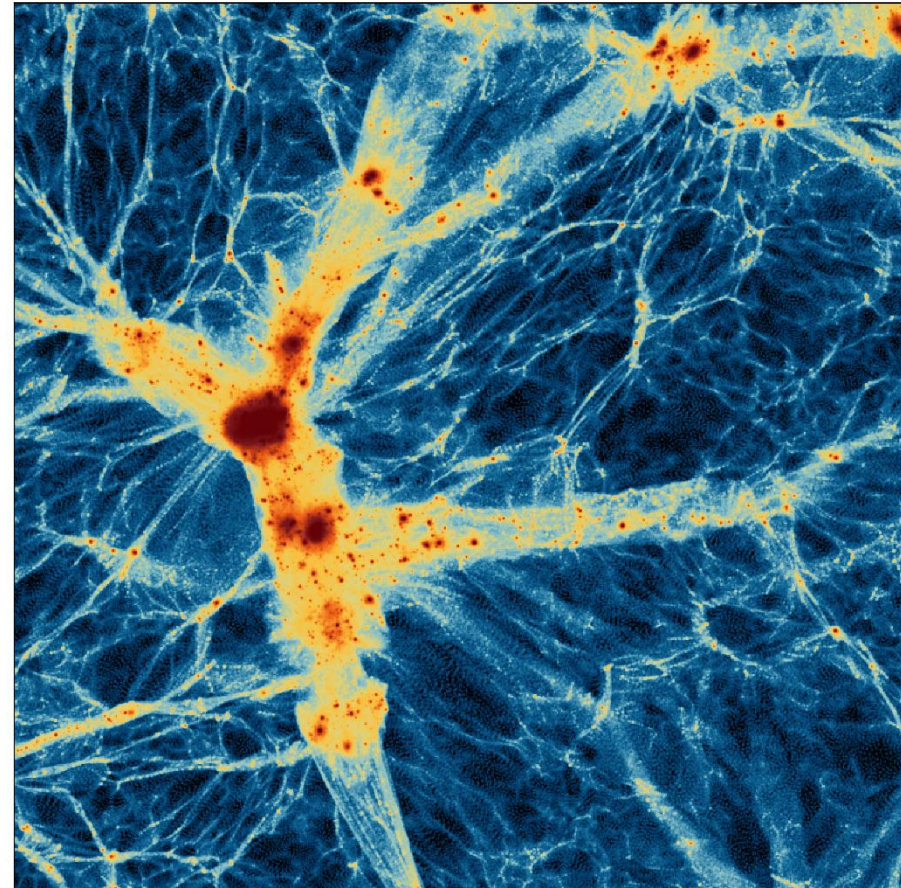


暗晕质量函数、暗晕形状、功率谱、  
双谱、.....

VS

纯暗物质N体 (DMO) 模拟

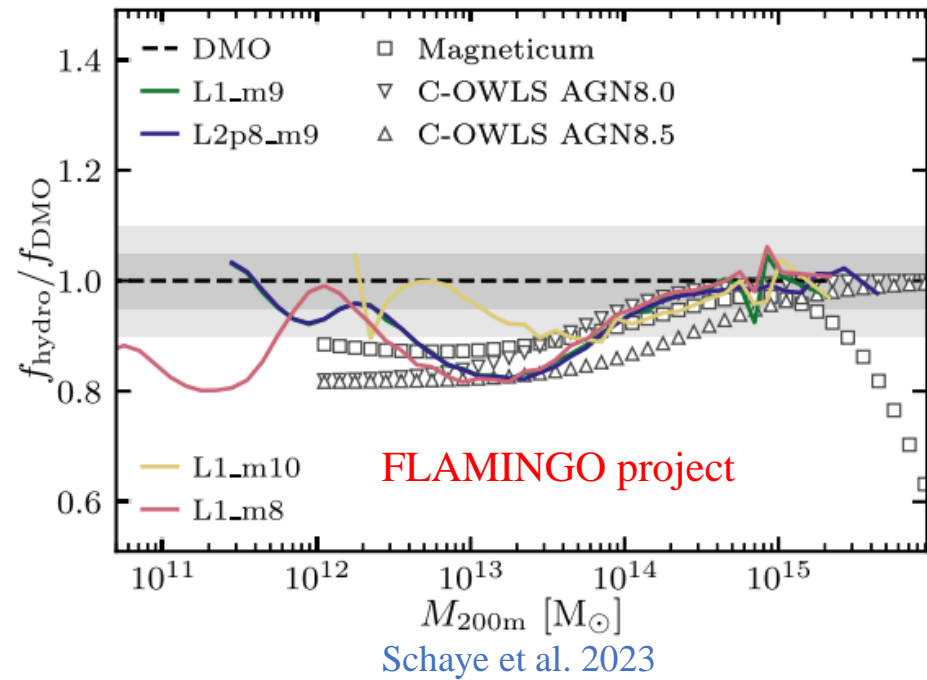
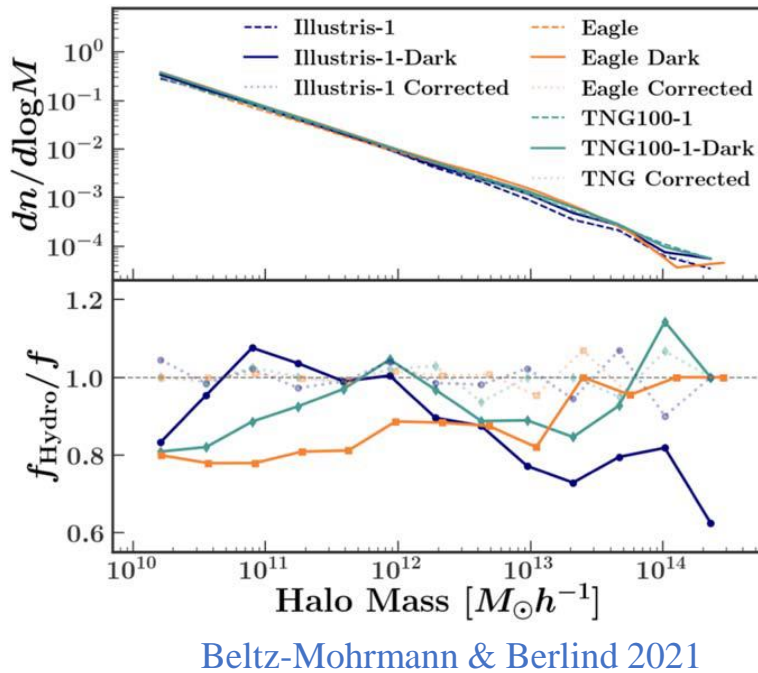
暗物质



暗晕质量函数、暗晕形状、功率谱、  
双谱、.....

# 重子效应的研究现状

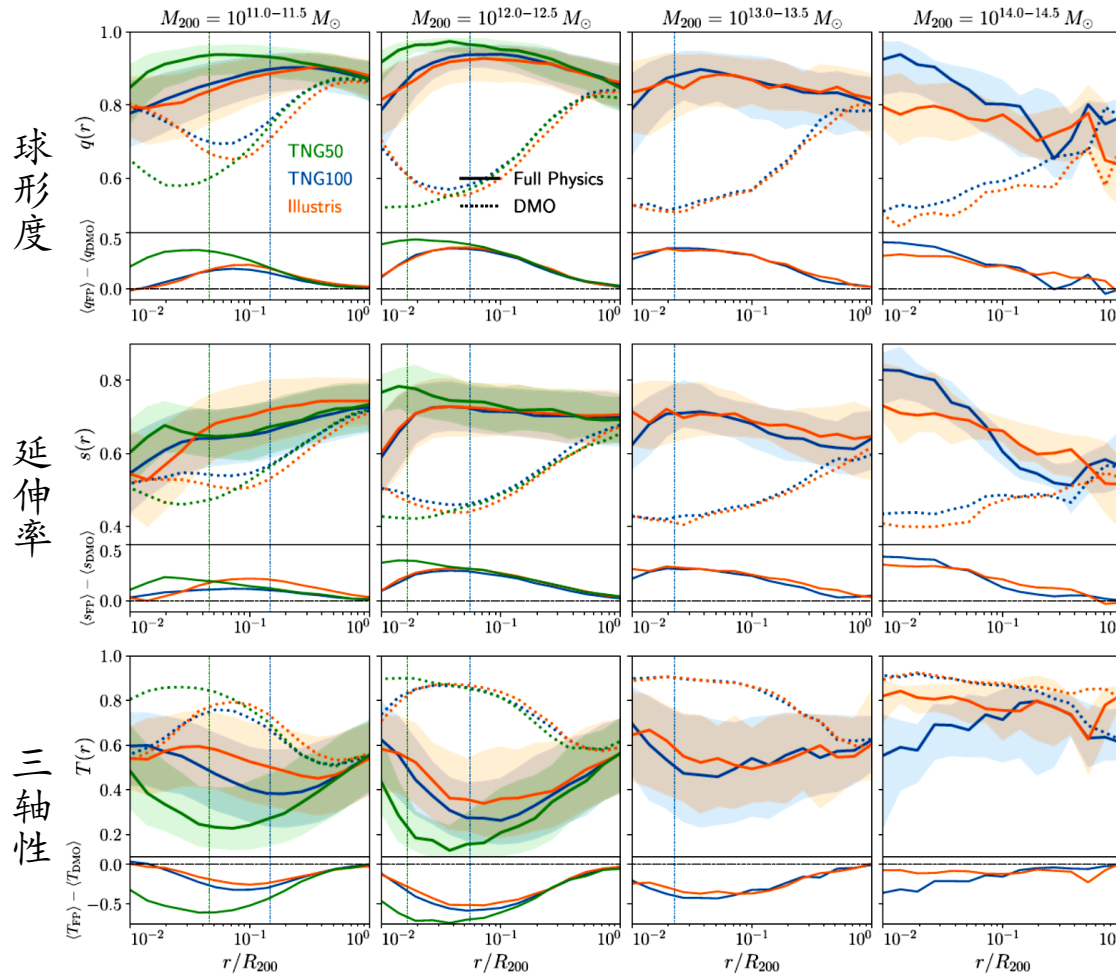
## 暗晕质量函数 (dark matter halo mass function)



- 相比于DMO模拟，流体模拟的暗晕质量函数降低~ 20%

# 重子效应的研究现状

## 暗晕形状 (dark matter halo shape)

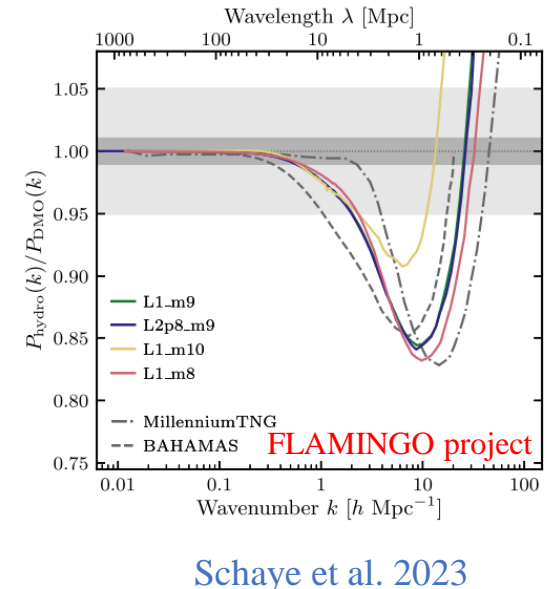
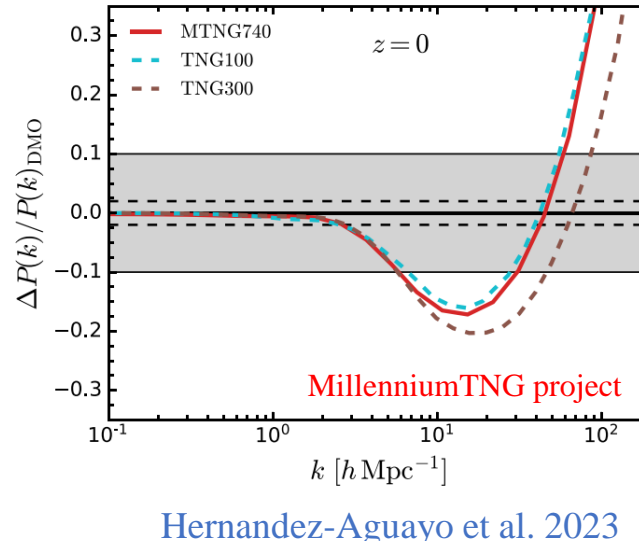
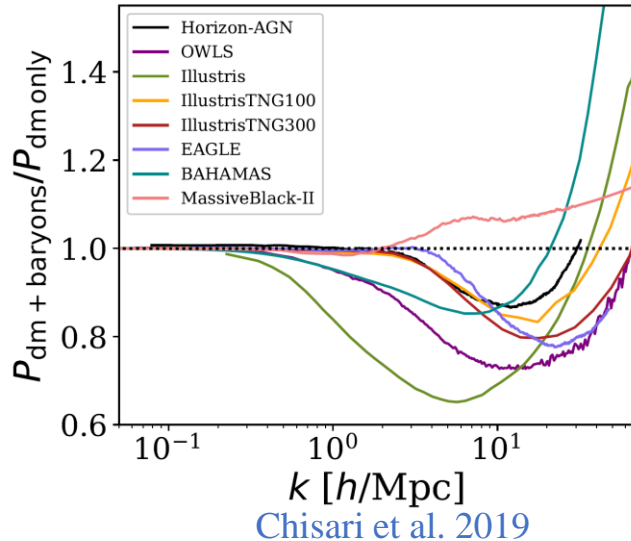


Chua et al. 2022

- 相比于DMO模拟，流体模拟的暗物质晕更加扁圆

# 重子效应的研究现状

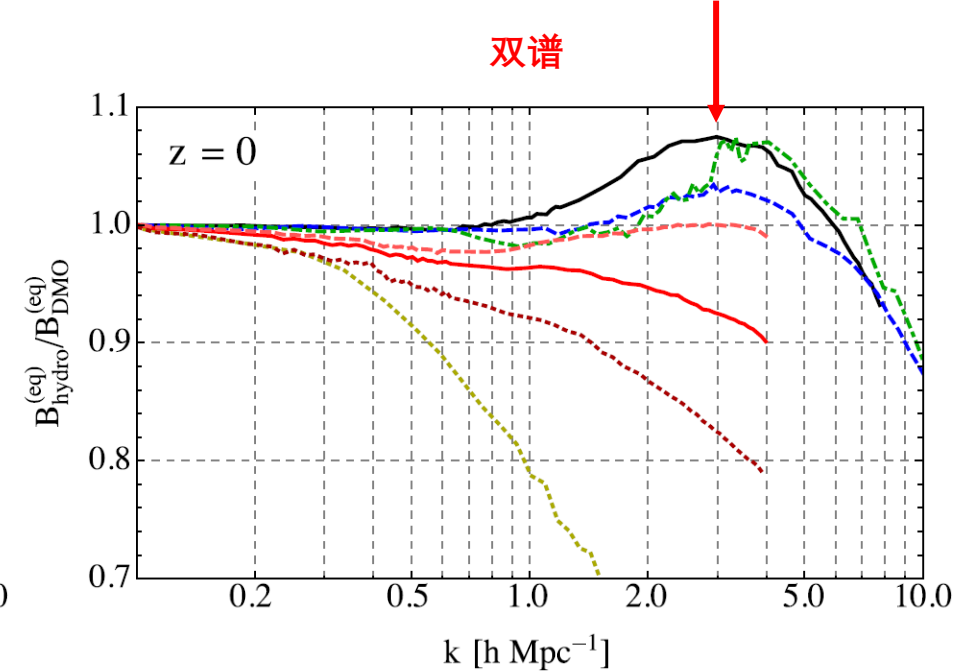
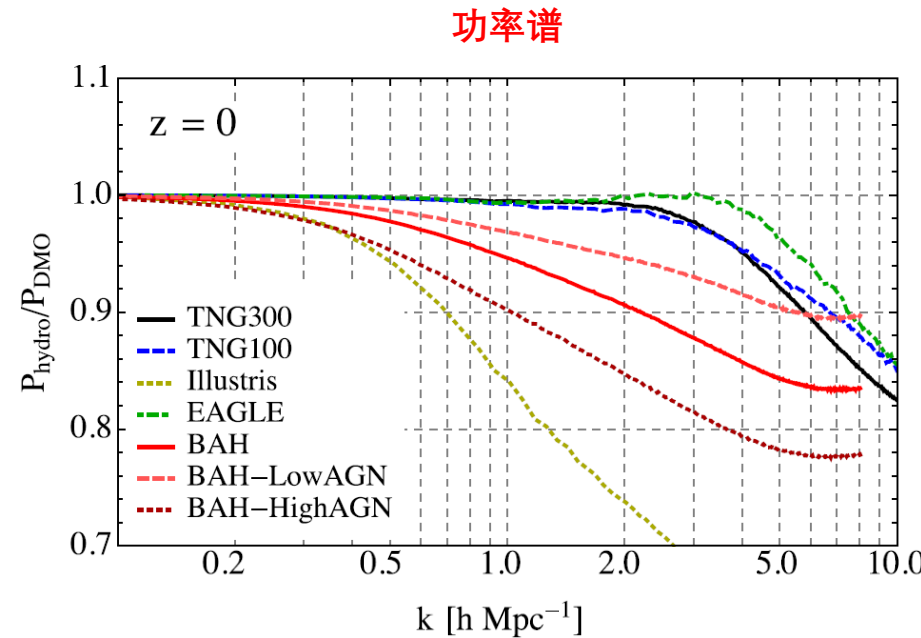
## 功率谱 (power spectrum)



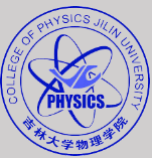
- 相比于DMO模拟，流体模拟的功率谱在  $k \sim 0.1 h \text{ Mpc}^{-1}$  开始减弱，幅度约  $\sim 1\%$ ；
- 随着  $k$  增大，减弱程度逐渐加深，并在  $k \sim 10 - 20 h \text{ Mpc}^{-1}$  达到  $\sim 20\%$ ；
- 当  $k > 20 h \text{ Mpc}^{-1}$ ，减弱趋势逐渐变小，流体模拟的功率谱转而增强

# 重子效应的研究现状

## 双谱 (bispectrum)



- 相比于DMO模拟，流体模拟的双谱在 $k \sim 3 \text{ h Mpc}^{-1}$ 受到明显增强



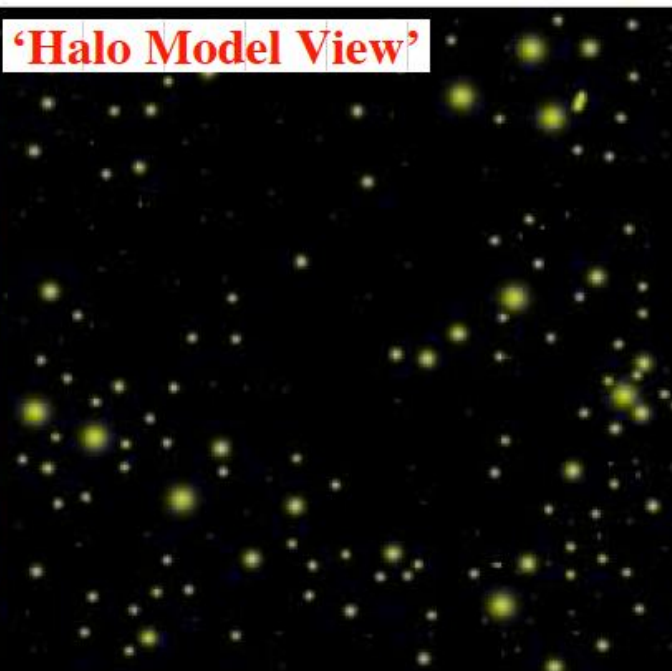
# 重子效应的研究现状

暗晕质量函数

暗晕形状

功率谱

双谱



假设宇宙物质全部位于暗晕内

# 重子效应的研究现状

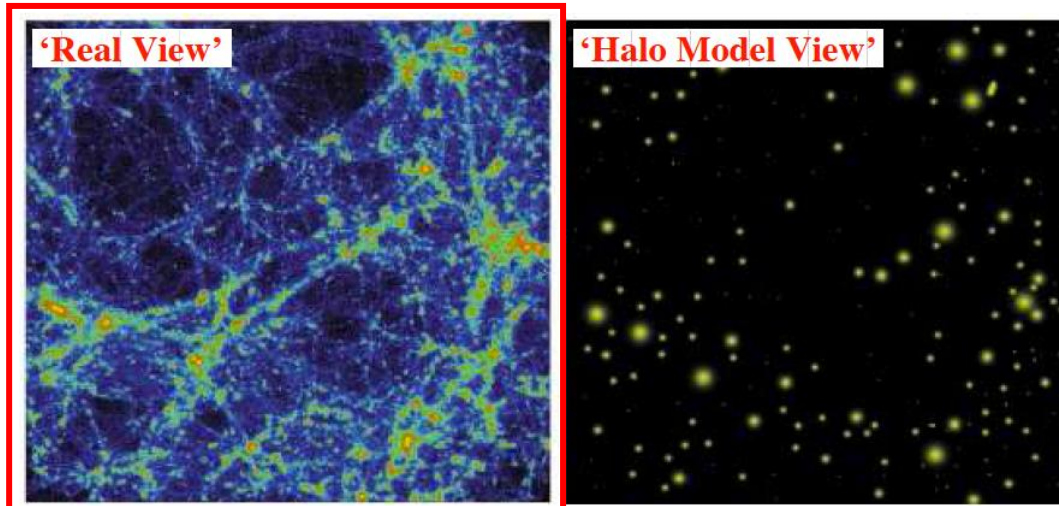
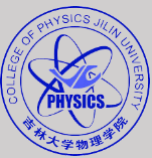


**Table 1.** Mass fraction of dark matter and baryons inside haloes at  $z = 0$ . The mass fractions are given with respect to the total mass inside the simulation volume. The first row shows the fractions for all haloes in the Illustris full physics simulation. The second row gives the mass contribution of haloes with a total mass higher than  $5 \times 10^9 M_\odot$  and the third and fourth rows show the respective values for haloes more massive than  $10^{12} M_\odot$  and  $10^{13} M_\odot$ , respectively. The last row gives the mass fraction for all haloes of the non-radiative Illustris run (no star formation, feedback or cooling).

	Per cent of total dark matter mass	Per cent of total baryonic mass			Per cent of total mass
		baryons	gas	stars	
All haloes	50.4 per cent	21.3 per cent	14.7 per cent	6.6 per cent	45.5 per cent
$M_{\text{tot}} > 5 \times 10^9 M_\odot$	44.6 per cent	21.3 per cent	14.7 per cent	6.6 per cent	40.7 per cent
$M_{\text{tot}} > 10^{12} M_\odot$	29.3 per cent	9.8 per cent	4.8 per cent	5.0 per cent	26.0 per cent
$M_{\text{tot}} > 10^{13} M_\odot$	20.1 per cent	7.2 per cent	4.0 per cent	3.2 per cent	18.0 per cent
$M_{\text{tot}} > 10^{14} M_\odot$	11.8 per cent	6.0 per cent	3.7 per cent	2.3 per cent	10.8 per cent
All haloes, non-radiative run	49.8 per cent	39.1 per cent		—	48.0 per cent

Haider et al. 2016



# 重子效应的研究现状

## Effects of Baryonic Feedback on the Cosmic Web

James Sunseri \*

<sup>1</sup>*Department of Astronomy, University of California, Berkeley, CA 94720-3411, USA*

<sup>2</sup>*Department of Physics, University of California, Berkeley, CA 94720-7300, USA*

Zack Li 

*Canadian Institute for Theoretical Astrophysics, University of Toronto, Toronto, ON, Canada M5S 3H8*

Jia Liu 

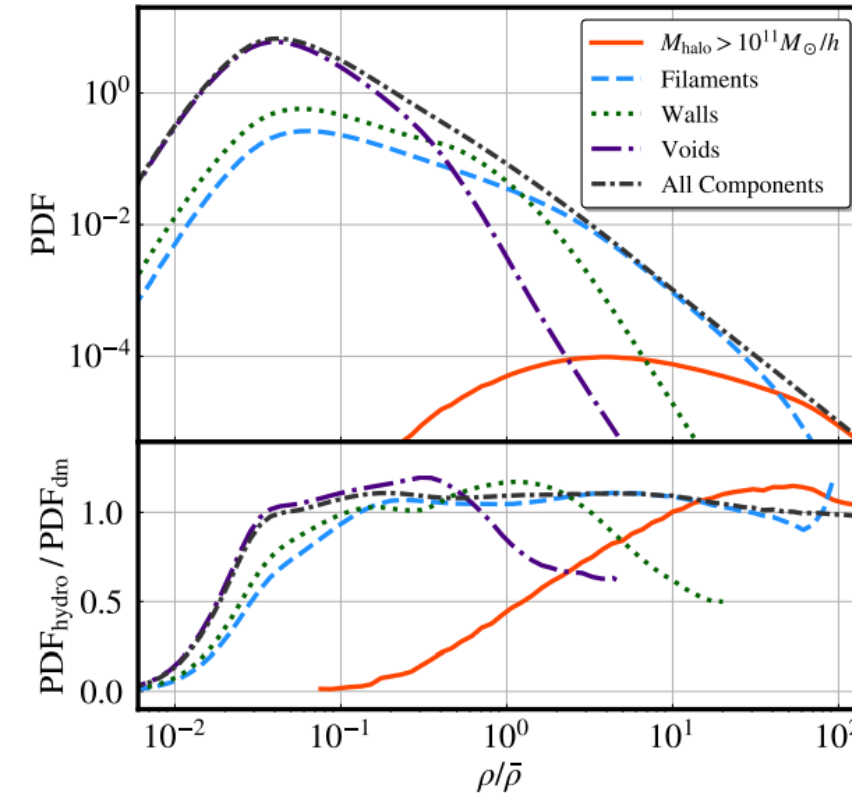
*Kavli IPMU (WPI), UTIAS, The University of Tokyo, Kashiwa, Chiba 277-8583, Japan*

(Dated: December 13, 2022)

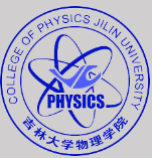
We study the effect of baryons on the cosmic web — halos, filaments, walls, and voids. To do so, we apply a modified version of NEXUS, a cosmic web morphological analysis algorithm, to the IllustrisTNG simulations. We find that halos lose more than 10% of their mass due to baryons, mostly to filaments and a small portion to walls and voids. However, the mass transfer does not significantly shift the boundaries of structures, leaving the volume fractions of the cosmic structures largely unaffected. We quantify the effects of baryonic feedback on the power spectrum and the probability density function (PDF) of the density field for individual cosmic structures. For the power spectrum, most suppression due to feedback can be accounted for by including  $M \geq 10^{12} M_{\odot}/h$  halos, without considering other cosmic structures. However, when examining the PDF of the density field, we find nearly 100% suppression of the emptiest regions and 10%-level effects (boost or suppression) in the remaining regions of filaments, walls, and voids. Our results indicate the importance of modeling the effects of baryons in the whole cosmic web, not just halos, for cosmological analysis beyond two-point statistics or field-based inferences. Our code is available through [COSMOMMF GITHUB](#).

DOI: [10.1103/PhysRevD.107.023514](https://doi.org/10.1103/PhysRevD.107.023514)

# 重子效应的研究现状



探究重子物理对整个宇宙结构的作用和影响，而不仅仅只考虑暗晕这一种结构，可能是未来研究的重要方向



# 重子效应的空间-尺度分析

Monthly Notices  
of the  
ROYAL ASTRONOMICAL SOCIETY

MNRAS 528, 3797–3808 (2024)  
Advance Access publication 2024 February 2



<https://doi.org/10.1093/mnras/stae229>

## How do baryonic effects on the cosmic matter distribution vary with scale and local density environment?

Yun Wang <sup>1</sup> and Ping He <sup>1,2</sup>

<sup>1</sup>College of Physics, Jilin University, Changchun 130012, China

<sup>2</sup>Center for High Energy Physics, Peking University, Beijing 100871, China

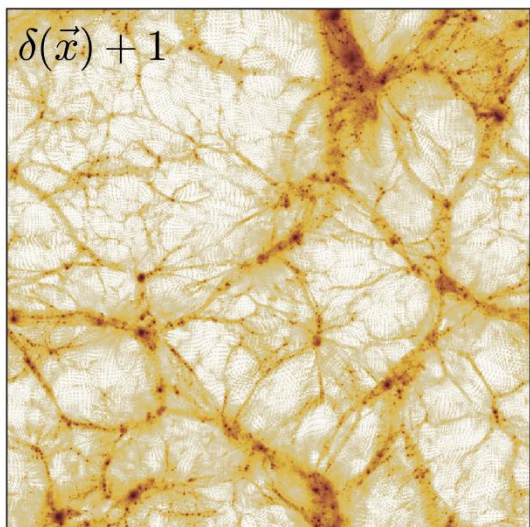
Accepted 2024 January 18. Received 2024 January 18; in original form 2023 October 31

### ABSTRACT

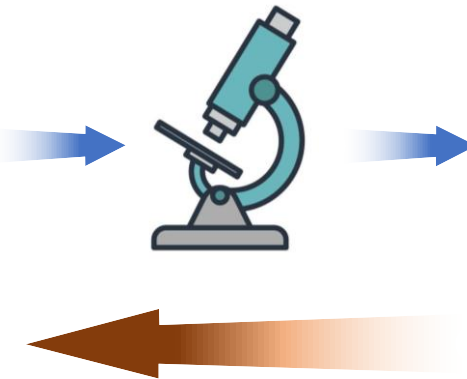
In this study, we investigate how the baryonic effects vary with scale and local density environment mainly by utilizing a novel statistic, the environment-dependent wavelet power spectrum (env-WPS). With four state-of-the-art cosmological simulation suites, EAGLE (Evolution and Assembly of GaLaxies and their Environments), SIMBA, Illustris, and IllustrisTNG, we compare the env-WPS of the total matter density field between the hydrodynamic and dark matter-only runs at  $z = 0$ . We find that the clustering is most strongly suppressed in the emptiest environment of  $\rho_m/\bar{\rho}_m < 0.1$  with maximum amplitudes  $\sim 67\text{--}89$  per cent on scales  $\sim 1.86\text{--}10.96 \text{ } h\text{Mpc}^{-1}$ , and less suppressed in higher density environments on small scales (except Illustris). In the environments of  $\rho_m/\bar{\rho}_m \geq 0.316$  ( $\geq 10$  in EAGLE), the feedbacks also lead to enhancement features at intermediate and large scales, which is most pronounced in the densest environment of  $\rho_m/\bar{\rho}_m \geq 100$  and reaches a maximum  $\sim 7\text{--}15$  per cent on scales  $\sim 0.87\text{--}2.62 \text{ } h\text{Mpc}^{-1}$  (except Illustris). The baryon fraction of the local environment decreases with increasing density, denoting the feedback strength, and potentially explaining some differences between simulations. We also measure the volume and mass fractions of local environments, which are affected by  $\gtrsim 1$  per cent due to baryon physics. In conclusion, our results show that the baryonic processes can strongly modify the overall cosmic structure on the scales of  $k > 0.1 \text{ } h\text{Mpc}^{-1}$ , which encourages further research in this direction.

DOI: [10.1093/mnras/stae229](https://doi.org/10.1093/mnras/stae229)

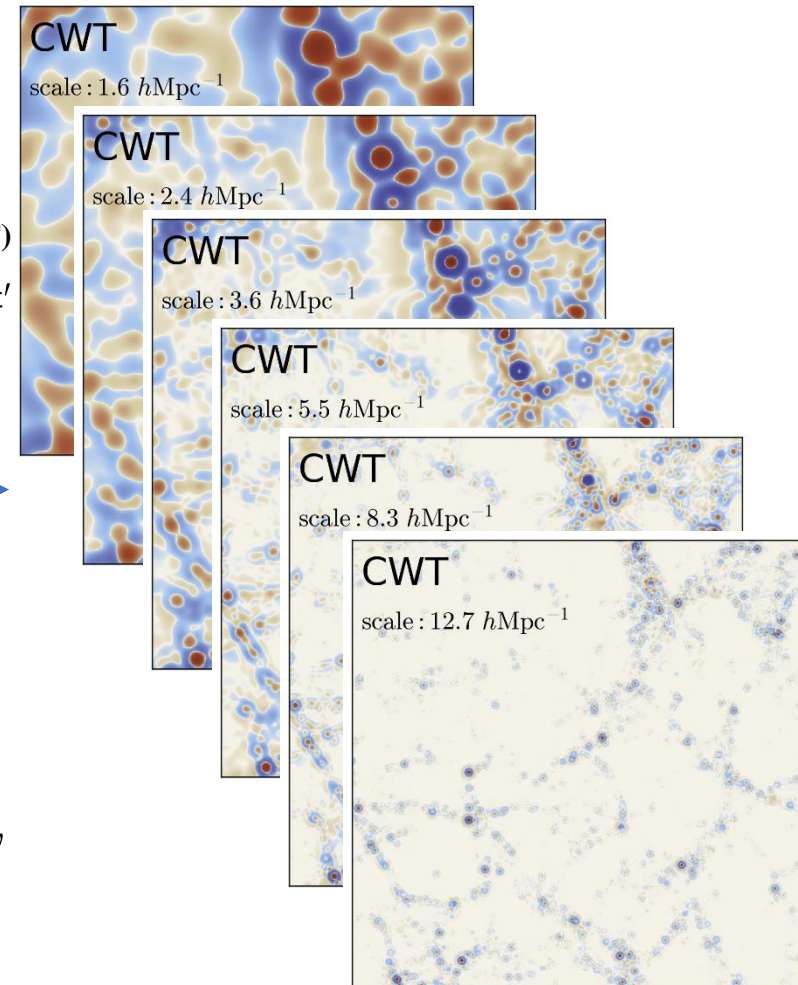
# 重子效应的空间-尺度分析

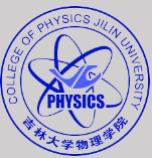


**连续小波变换**  
(continuous wavelet transform, CWT)  
 $\tilde{\delta}(w, \mathbf{x}) = \int \delta(\mathbf{x}') \Psi(w, \mathbf{x} - \mathbf{x}') d^3 \mathbf{x}'$



$$\delta(\mathbf{x}) = \frac{1}{\mathcal{K}_\Psi} \int_0^{+\infty} w^{\frac{1}{2}} \tilde{\delta}(w, \mathbf{x}) dw$$





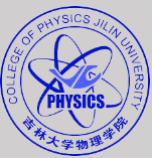
# 重子效应的空间-尺度分析

环境依赖的小波功率谱

(environment-dependent Wavelet Power Spectrum, env-WPS)

env-WPS

$$\tilde{P}(w, \delta) \equiv \left\langle \left| \tilde{\delta}(w, \mathbf{x}) \right|^2 \right\rangle_{\delta(\mathbf{x}) = \delta}$$



# 重子效应的空间-尺度分析

## 环境依赖的小波功率谱

(environment-dependent Wavelet Power Spectrum, env-WPS)

env-WPS

$$\tilde{P}(w, \delta) \equiv \left\langle \left| \tilde{\delta}(w, \mathbf{x}) \right|^2 \right\rangle_{\delta(\mathbf{x}) = \delta}$$

global-WPS

$$\tilde{P}(w) = \left\langle \left| \tilde{\delta}(w, \mathbf{x}) \right|^2 \right\rangle_{\text{all } \delta} = \left\langle \left| \tilde{\delta}(w, \mathbf{x}) \right|^2 \right\rangle_V$$

global-WPS & env-WPS

$$\tilde{P}(w) = \sum_{\delta} f_V(\delta) \tilde{P}(w, \delta)$$

# 重子效应的空间-尺度分析

## 环境依赖的小波功率谱

(environment-dependent Wavelet Power Spectrum, env-WPS)

env-WPS

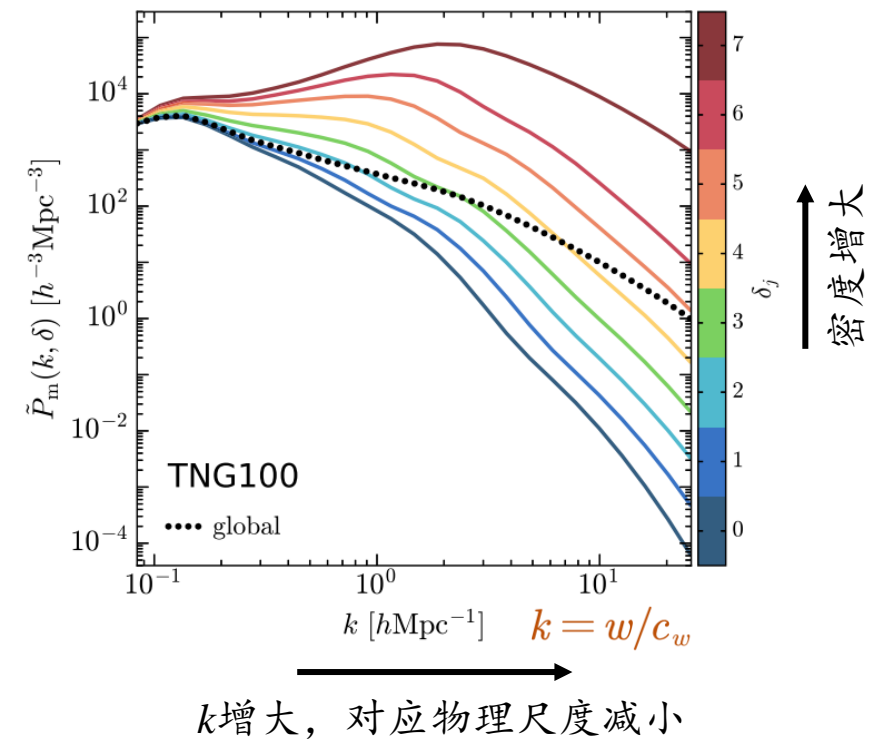
$$\tilde{P}(w, \delta) \equiv \left\langle |\tilde{\delta}(w, \mathbf{x})|^2 \right\rangle_{\delta(\mathbf{x}) = \delta}$$

global-WPS

$$\tilde{P}(w) = \left\langle |\tilde{\delta}(w, \mathbf{x})|^2 \right\rangle_{\text{all } \delta} = \left\langle |\tilde{\delta}(w, \mathbf{x})|^2 \right\rangle_V$$

global-WPS & env-WPS

$$\tilde{P}(w) = \sum_{\delta} f_V(\delta) \tilde{P}(w, \delta)$$



# 重子效应的空间-尺度分析

## 重子效应的测定

流体模拟中 env-WPS 与相应  
N 体模拟中 env-WPS 的相对偏差

$$R(k, \delta) = \frac{\tilde{P}_{\text{Hydro}}(k, \delta)}{\tilde{P}_{\text{DMO}}(k, \delta)} - 1$$

global-WPS 的相对偏差

$$\begin{aligned} R(k) &= \frac{\tilde{P}_{\text{Hydro}}(k)}{\tilde{P}_{\text{DMO}}(k)} - 1 \\ &= \sum_{\delta} f_{\text{V}}^{\text{Hydro}}(\delta) \tilde{P}_{\text{Hydro}}(k) / \tilde{P}_{\text{DMO}}(k) - 1 \\ &= \sum_{\delta} [r_{\text{V}}(\delta) + 1] [R(k, \delta) + 1] Q_{\text{DMO}}(k, \delta) - 1 \end{aligned}$$

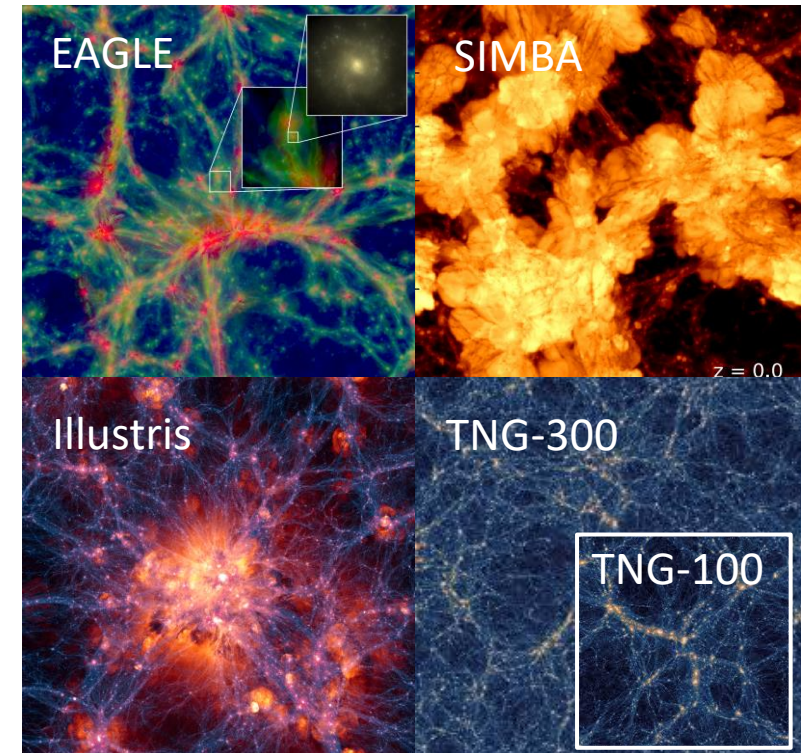
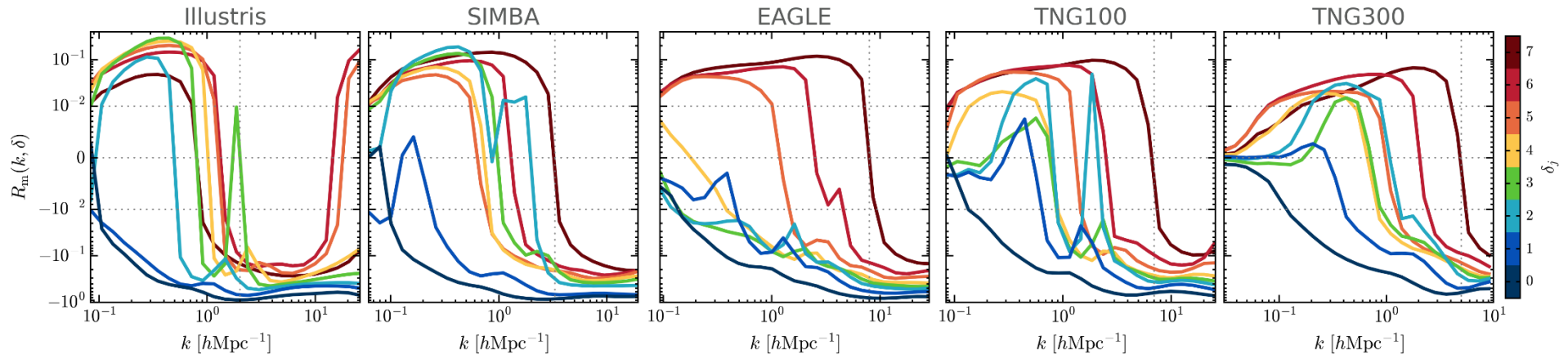


**Table 2.** The local density environments.

	$\delta_0$	$\delta_1$	$\delta_2$	$\delta_3$	$\delta_4$	$\delta_5$	$\delta_6$	$\delta_7$
$\delta_m \in$	[-1, -0.9)	[-0.9, -0.684)	[-0.684, 0)	[0, 2.162)	[2.162, 9)	[9, 30.623)	[30.623, 99)	[99, $+\infty$ )
$\rho_m / \bar{\rho}_m \in$	[0, 0.1)	[0.1, 0.316)	[0.316, 1)	[1, 3.162)	[3.162, 10)	[10, 31.623)	[31.623, 100)	[100, $+\infty$ )

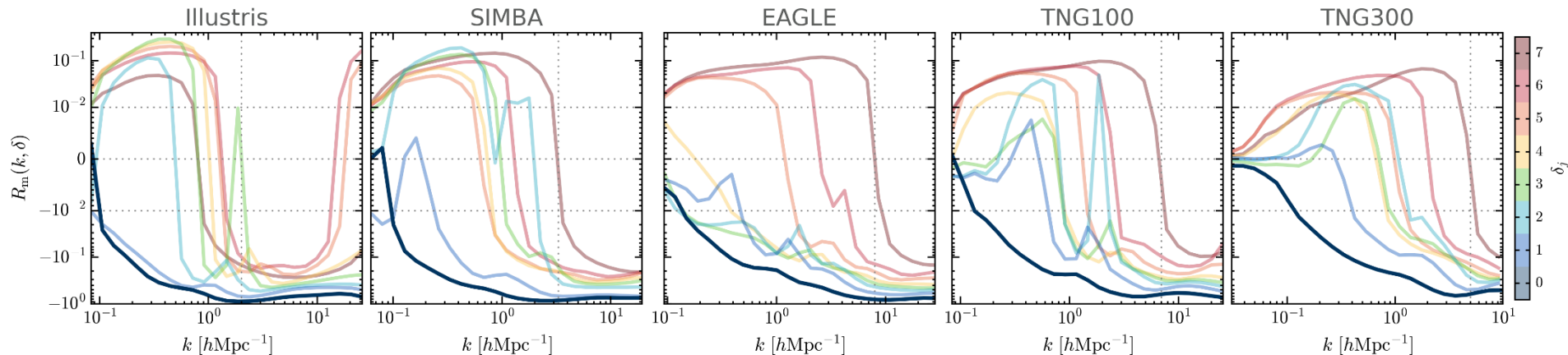
# 结果和结论

- 在  $k \sim 0.1 h \text{ Mpc}^{-1}$ , 大部分密度环境中的物质成团强度改变了  $\sim 1\%$



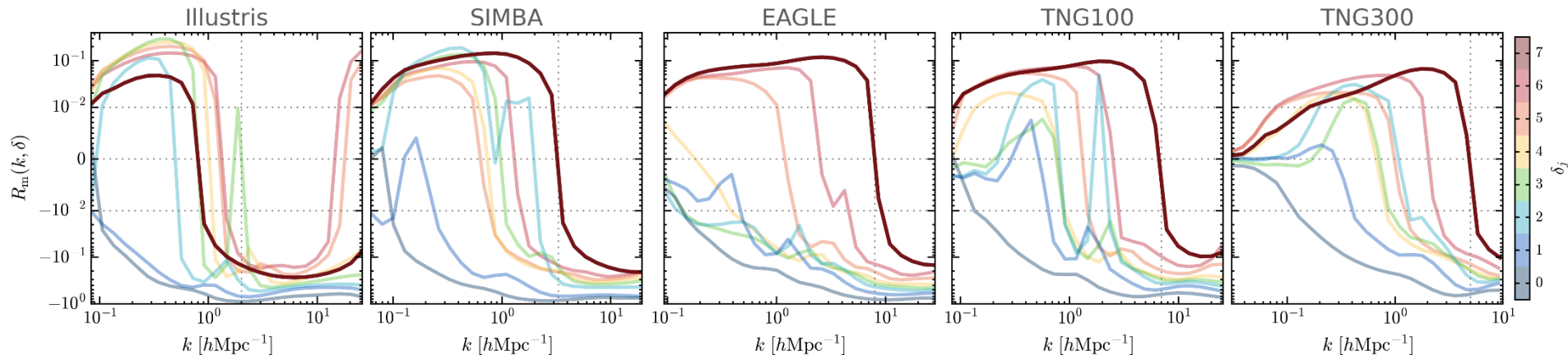
# 结果和结论

- 在  $k \sim 0.1 h \text{ Mpc}^{-1}$ , 大部分密度环境中的物质成团强度改变了  $\sim 1\%$
- 在  $\rho/\bar{\rho} < 0.1 (\delta_0)$  的欠密度环境, 物质成团在  $1.86 - 10.96 h \text{ Mpc}^{-1}$  的尺度范围被抑制了  $67 - 89\%$ ; 在  $\rho/\bar{\rho} > 0.1$  的密度环境, 抑制程度随着密度增高而减小



# 结果和结论

- 在  $k \sim 0.1 h \text{ Mpc}^{-1}$ , 大部分密度环境中的物质成团强度改变了  $\sim 1\%$
- 在  $\rho/\bar{\rho} < 0.1 (\delta_0)$  的欠密度环境, 物质成团在  $1.86 - 10.96 h \text{ Mpc}^{-1}$  的尺度范围被抑制了  $67 - 89\%$ ; 在  $\rho/\bar{\rho} > 0.1$  的密度环境, 抑制程度随着密度增高而减小
- 在  $\rho/\bar{\rho} > 0.3 (\delta_{j \geq 2})$  的密度环境 (EAGLE:  $\rho/\bar{\rho} > 10$ ), 物质成团在中等及大尺度上得到增强
- 在  $\rho/\bar{\rho} > 100 (\delta_7)$  的最致密环境, 物质成团的增强幅度在  $0.87 - 2.62 h \text{ Mpc}^{-1}$  的尺度达到最大, 约为  $7 - 15\%$  (Illustris 除外)

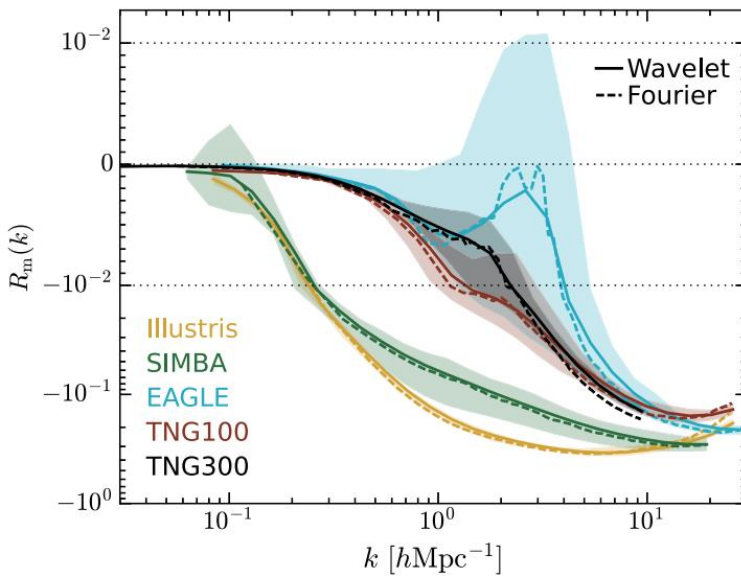


# 结果和结论

## global-WPS的相对偏差

$$\begin{aligned}
 R(k) &= \frac{\tilde{P}_{\text{Hydro}}(k)}{\tilde{P}_{\text{DMO}}(k)} - 1 \\
 &= \sum_{\delta} f_{\text{V}}^{\text{Hydro}}(\delta) \tilde{P}_{\text{Hydro}}(k) / \tilde{P}_{\text{DMO}}(k) - 1 \\
 &= \sum_{\delta} [r_{\text{V}}(\delta) + 1] [R(k, \delta) + 1] Q_{\text{DMO}}(k, \delta) - 1
 \end{aligned}$$

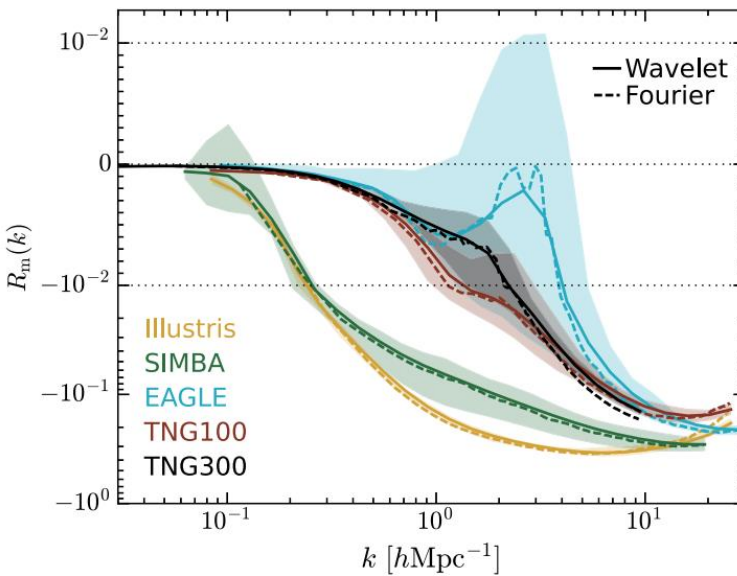
- global-WPS的抑制效应与傅里叶功率谱几乎完全等同



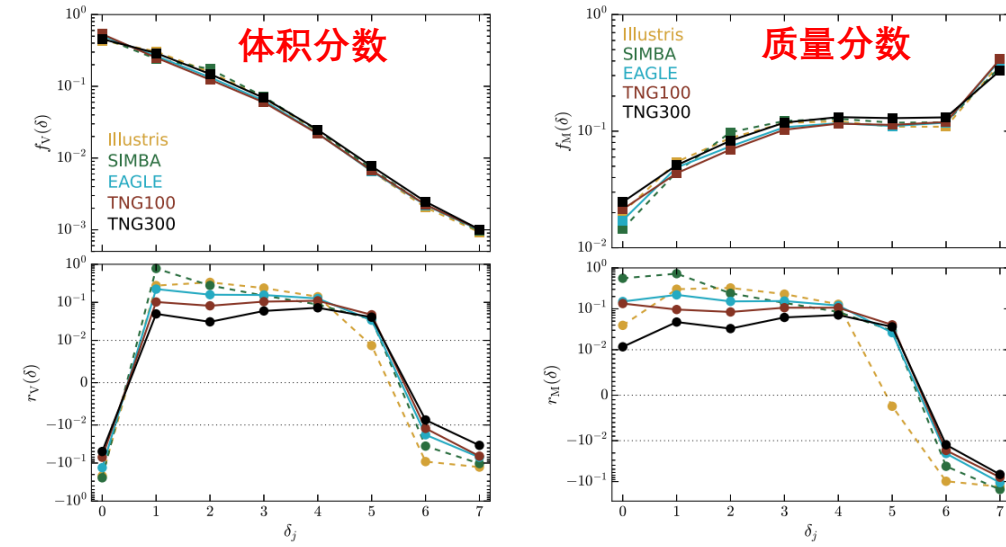
# 结果和结论

## global-WPS的相对偏差

$$\begin{aligned}
 R(k) &= \frac{\tilde{P}_{\text{Hydro}}(k)}{\tilde{P}_{\text{DMO}}(k)} - 1 \\
 &= \sum_{\delta} f_V^{\text{Hydro}}(\delta) \tilde{P}_{\text{Hydro}}(k) / \tilde{P}_{\text{DMO}}(k) - 1 \\
 &= \sum_{\delta} [r_V(\delta) + 1] [R(k, \delta) + 1] Q_{\text{DMO}}(k, \delta) - 1
 \end{aligned}$$



- global-WPS的抑制效应与傅里叶功率谱几乎完全等同
- 体积分数随着密度增大而减小
- 质量分数随着密度增大而增大
- 体积和质量的改变都  $\geq 1\%$

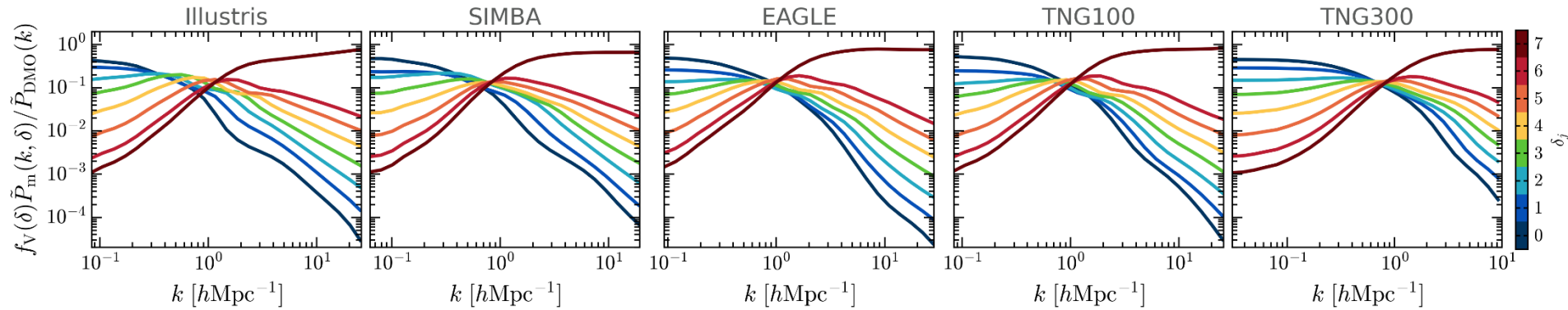


# 结果和结论

## global-WPS的相对偏差

$$\begin{aligned}
 R(k) &= \frac{\tilde{P}_{\text{Hydro}}(k)}{\tilde{P}_{\text{DMO}}(k)} - 1 \\
 &= \sum_{\delta} f_V^{\text{Hydro}}(\delta) \tilde{P}_{\text{Hydro}}(k) / \tilde{P}_{\text{DMO}}(k) - 1 \\
 &= \sum_{\delta} [r_V(\delta) + 1] [R(k, \delta) + 1] Q_{\text{DMO}}(k, \delta) - 1
 \end{aligned}$$

- 局部密度环境对global-WPS抑制效应的贡献量表现为“蝴蝶结”

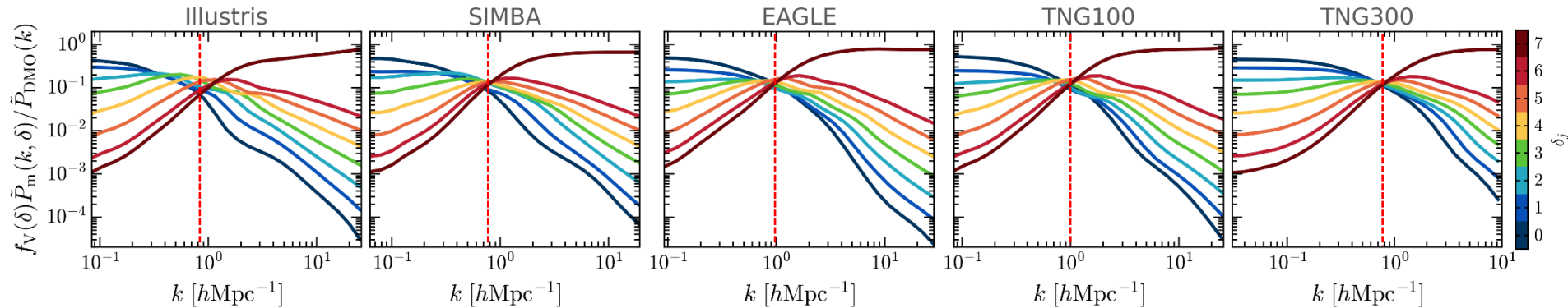


# 结果和结论

## global-WPS的相对偏差

$$\begin{aligned}
 R(k) &= \frac{\tilde{P}_{\text{Hydro}}(k)}{\tilde{P}_{\text{DMO}}(k)} - 1 \\
 &= \sum_{\delta} f_V^{\text{Hydro}}(\delta) \tilde{P}_{\text{Hydro}}(k) / \tilde{P}_{\text{DMO}}(k) - 1 \\
 &= \sum_{\delta} [r_V(\delta) + 1] [R(k, \delta) + 1] Q_{\text{DMO}}(k, \delta) - 1
 \end{aligned}$$

- 局部密度环境对global-WPS抑制效应的贡献量表现为“蝴蝶结”
- “蝴蝶结”的结点尺度 $k_{\text{knot}}$ 位于 $k \sim 1 h \text{ Mpc}^{-1}$

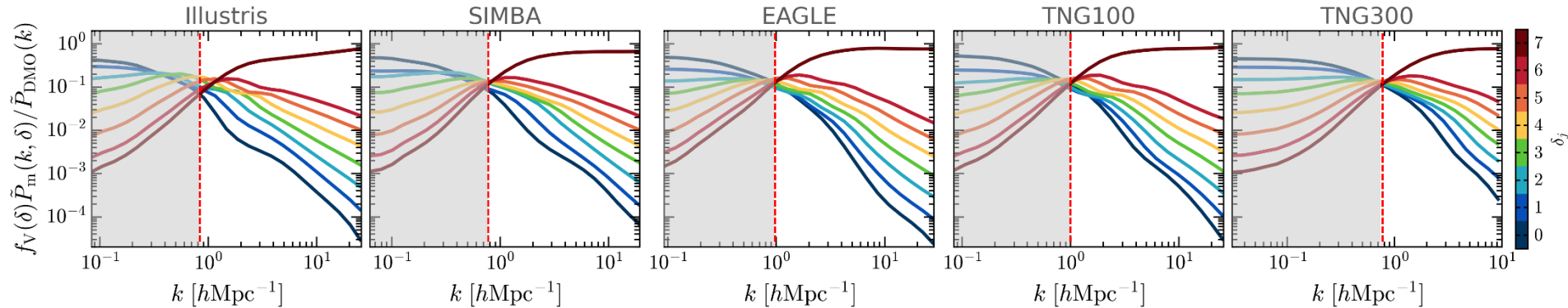


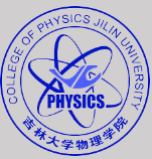
# 结果和结论

## global-WPS的相对偏差

$$\begin{aligned}
 R(k) &= \frac{\tilde{P}_{\text{Hydro}}(k)}{\tilde{P}_{\text{DMO}}(k)} - 1 \\
 &= \sum_{\delta} f_V^{\text{Hydro}}(\delta) \tilde{P}_{\text{Hydro}}(k) / \tilde{P}_{\text{DMO}}(k) - 1 \\
 &= \sum_{\delta} [r_V(\delta) + 1] [R(k, \delta) + 1] Q_{\text{DMO}}(k, \delta) - 1
 \end{aligned}$$

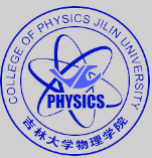
- 局部密度环境对global-WPS抑制效应的贡献量表现为“蝴蝶结”
- “蝴蝶结”的结点尺度 $k_{\text{knot}}$ 位于 $k \sim 1 h \text{ Mpc}^{-1}$
- $k < k_{\text{knot}}$ : global-WPS的抑制主要来自大体积的欠密度环境(空洞)
- $k > k_{\text{knot}}$ : global-WPS的抑制主要来自大质量的致密环境(暗晕)





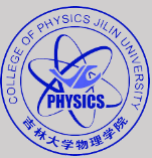
# 总结和展望

- 在  $k > 0.1h \text{ Mpc}^{-1}$  的尺度，重子物理对所有的密度环境都产生了较显著的作用，而非只改变最致密环境的物质分布。



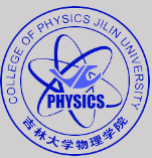
# 总结和展望

- 在  $k > 0.1h \text{ Mpc}^{-1}$  的尺度，重子物理对所有的密度环境都产生了较显著的作用，而非只改变最致密环境的物质分布。
- 更大体积的流体模拟：FLAMINGO、MillenniumTNG、……



# 总结和展望

- 在  $k > 0.1h \text{ Mpc}^{-1}$  的尺度，重子物理对所有的密度环境都产生了较显著的作用，而非只改变最致密环境的物质分布。
- 更大体积的流体模拟：FLAMINGO、MillenniumTNG、……
- 重子物理参数可调控、拥有大量随机实现的模拟：CAMELS



# 总结和展望

- 在  $k > 0.1h \text{ Mpc}^{-1}$  的尺度，重子物理对所有的密度环境都产生了较显著的作用，而非只改变最致密环境的物质分布。
- 更大体积的流体模拟：FLAMINGO、MillenniumTNG、……
- 重子物理参数可调控、拥有大量随机实现的模拟：CAMELS
- 更加稳健的宇宙结构分类方案：NEXUS、……

# 欢迎提问

